FLOW OF A FLUID THROUGH A POROUS SOLID DUE TO HIGH PRESSURE GRADIENTS

SHRIRAM SRINIVASAN, ANDREA BONITO, AND K. R. RAJAGOPAL

Abstract. It is well known that the viscosity of fluids could vary by several orders of magnitude with pressure. This fact is not usually taken into account in many important applications involving the flow of fluids through a porous media, like the problems of enhanced oil recovery or carbon dioxide sequestration where very high pressure differentials are involved. Another important technical problem where such high pressure differentials are involved is that of extracting unconventional oil deposits such as shale which is becoming ever so important now. In this study, we show that the traditional approach that ignores the variation of the viscosity and drag with the pressure greatly over-predicts the mass flux taking place through the porous structure. While taking the pressure dependence of viscosity and drag leads to a ceiling flux, the traditional approaches lead to a continued increase in the flux with the pressure difference. In this study, we consider a generalization of the classical Brinkman equation that takes the dependence of the viscosity and the Drag coefficient on pressure. To our knowledge, this is the first study to carry out such an analysis.

1. Introduction

Darcy's equation [1] is the most popular mathematical model to describe the flow of fluids through a porous solid due to an applied pressure gradient. Darcy's equation, which is commonly referred to as "Darcy's law" is an approximation that is valid only if numerous assumptions are met (See Munaf *et al* [2], Rajagopal [3]). Far from being a "law" with universal or for that matter wide ranging applicability, the classical Darcy's equation, which is an approximation to the balance of linear momentum is reasonable only if

(1) The solid is a rigid porous body whose balance of linear momentum can be ignored. The stresses developed in the rigid solid body being that which is necessary to meet the balance of linear momentum.
(2) The pore structure in the solid is uniform and hence there is no inhomogeneity in the pore structure.
(3) The flow is sufficiently slow so that the inertial effects in the fluid can be neglected.
(4) The frictional effects in the fluid due to the viscosity of the fluid can be neglected.

Date: Started: September 15, 2011; Updated: April 26, 2012.

Key words and phrases. pressure-dependent drag coefficient and viscosity; porous rigid solid; Barus formula; Brinkman model; Darcy equation; Stokes equation.

(5) The only interaction between the solid and the fluid is due to the friction at the pores and is proportional to the relative velocity between the solid and the fluid.

(6) The flow is steady.

(7) The fluid is incompressible.

(8) The pressure range that the fluid is subject to does not lead to changes in the viscosity of the fluid.

(9) The partial stress in the fluid is that in an Euler fluid.

In this paper, we are interested in the flow of a fluid through a porous solid when assumptions (4),(8) and (9) do not hold. Such flows have relevance to several problems in petroleum and geotechnical engineering, for example problems such as enhanced oil recovery and carbon di-oxide sequestration where the range of pressure that the fluid is subject to is very large. In some of the problems, more than one fluid is involved such as steam and oil in enhanced oil recovery. However before embarking on the study of such problems, it is necessary to study the problem of a single fluid flowing through a porous solid. When assumption (4) alone does not hold, we obtain the equations developed by Brinkman [4, 5].

That the viscosity of the fluid can depend on pressure is very well established. The history of the early experimental results concerning the same can be found in the book by Bridgman [6] on the physics of high pressure. Stokes [7] was aware of the viscosity of the fluid depending on the pressure and as early as 1893 Barus [8] suggested an exponential dependence of the viscosity on the pressure based on his experimental investigations. Bridgman [6] in his book cites a personal communication from Andrade that provides a relationship of the viscosity to the temperature, density and pressure [1] (see also the discussion in [10]). There has been a great deal of experimental data since Bridgman's book that document the variation of viscosity with pressure (see [11, 12, 13, 14, 15, 16, 17, 18, 19, 20, 21, 22]). In most liquids, while the variation in the viscosity can be of the order of 10^8 (see Bair and Kottke [21]), the variation of the density due to variation in the pressure is of the order of a few percent (see Dowson and Higginson [23], Rajagopal [24]), and thus it would be reasonable to assume that the liquid is incompressible while the visocity varies with the pressure. The variation of the viscosity with the pressure implies that the "Drag coefficient that appears in the equations governing the flow of a liquid through a porous solid will depend on the pressure.

In this study, while we assume that the viscosity and "Drag coefficient" depend on the pressure, we assume that the other assumptions mentioned above hold. This leads to a generalization of the Brinkman equation with the viscosity and the "Drag coefficient" depending upon the pressure.

[1] Despite our attempts to locate the paper by Andrade wherein that formula is given, we have been unable to do so. The reference to Andrade [9] that Bridgman provides does not contain the formula mentioned.

Recently, Nakshatrala and Rajagopal [25] studied the generalization of Darcy's equation when the "Drag coefficient" depends on the pressure.

As we mentioned earlier, Barus [8] suggested an exponential dependence of the viscosity on the pressure, i.e.,

$$\mu(p) = \mu_0 \exp(\beta p), \quad \mu_0 > 0,\ \beta \geq 0, \tag{1.1}$$

where μ_0 and β are constants , with μ_0 having the dimension of viscosity and β the dimension that is the inverse of that of the pressure. The expression (1.1) would lead to a "Drag coefficient" $\alpha(p)$ of the form

$$\alpha(p) = \alpha_0 \exp(\beta p), \quad \alpha_0 \geq 0, \tag{1.2}$$

where α_0 is a constant with dimension of $\mathrm{ML}^{-3}\mathrm{T}^{-1}$.

Using a semi-inverse approach, Kannan and Rajagopal [26] studied the flow of a fluid through a porous inclined slab. They considered a variety of forms for the dependence of viscosity and the "Drag coefficient" including the exponential dependence given in (1.1), (1.2). We shall not get into a detailed discussion of their results, suffice it is to say the solutions exhibited markedly different characteristics than the solutions for the classical Darcy and Brinkman equations. The semi-inverse solution sought simplifies the problem greatly and the governing equations reduce to a simple ordinary differential equation.

Recently, Nakshatrala and Rajagopal [25] were able to study numerically the problem corresponding to the generalization of Darcy's equation, when the "Drag coefficient" depends exponentially on the pressure as given in (1.2). They were able to find solutions to the partial differential equation governing the flow using a mixed finite element method. They showed that the results they obtain are different from the solution to the classical Darcy's equation. Assuming that the "Drag coefficient" is a bounded function of the pressure in the generalized Darcy's equation, Girault *et al* [27] guaranteed the well-posedness of the system together with the convergence of a finite element method. When the dependence on the pressure is exponential (as in (1.2), the authors propose an interesting splitting algorithm, observed numerically to be robust in the parameter range tested.

The generalization of the Brinkman equation considered here (viscosity and "Drag coefficient" given by (1.1) and (1.2) respectively), no theoretical convergence results are available. While we are unable to obtain a numerical solution of the governing equations for large values of the non-dimensionalized pressure-viscosity coefficient "β" that appears in the viscosity-pressure relation (1.1) , we are however able to obtain solutions to the problem when the non-dimensionalized pressure-viscosity coefficient $\bar{\beta}$ is small. Fortunately, for the class of incompressible fluids (like mineral oil for instance) that we are interested in, the non-dimensionalized pressure-viscosity coefficient $\bar{\beta}$ is indeed small (see Section 4 for details).

It is worth noting that the viscosity data for various pressures have been obtained from experiments where the applied pressure is positive, i.e., the applied normal stress is compressive. When the pressure is sufficiently low cavitation can occur, leading to the formation of cavities or bubbles in the flow field. Cavitation is the phenomenon that occurs at sufficiently low pressure, when the pressure of the fluid at the location becomes less than the vapor pressure of the liquid at that temperature at the location in question. Cavitation occurs in the flows of fluids through pumps, bearings and adjacent to rotating propellers amongst other flows. The "Drag" due to the motion of a solid in a cavitating fluid is not well understood and more importantly there is no measurement of the viscosity of fluids in such a state. In view of this, we shall adopt a procedure that is followed in lubrication and assume that when the pressure becomes negative the viscosity corresponds to that for zero pressure (see Szeri [28] for a detailed discussion of the manner in which cavitation is handled within the context of obtaining numerical solutions in elastohydrodynamics wherein very high pressures are involved). For the fluids considered here, we shall assume that the variation of viscosity and "Drag coefficient" is negligible when the pressure is negative and that both the viscosity and "Drag coefficient" are a continuous function of the pressure. Furthermore, the numerical method used requires that the function be differentiable. In Appendix A the viscosity and "Drag coefficients" are chosen to be a particular smooth function of the pressure which satisfies all our hypotheses.

When $\beta = 0$, the problem reduces to that considered by Brinkman, namely the viscosity being constant.

When the viscosity and "Drag coefficient" is given by (1.1) and (1.2) respectively, we find that the volumetric flux due to the pressure gradient is distinctively and characteristically different. While the classical Brinkman equation predicts a linear relationship between the volumetric flux and the pressure gradient as the pressure gradient increases, the model employed in the study predicts a ceiling flux as the pressure gradient increases. One would expect such a relationship as one cannot push through more than a certain quantity of fluid. In fact, increasing the pressure gradient significantly will lead to the flow becoming turbulent with the possibility of back flow, leading in fact to the diminishing of the volumetric flux at very high pressure gradient. As is to be expected, we also find that as the pressure difference between the inlet and the outlet increases, the region wherein the component of the velocity is close to a constant decreases, that is, the effect of the no-slip velocity boundary condition is more pronounced when the pressure gradient causing the flow is larger. We also find that the component of the velocity in the direction normal to the gradient (see Figure 1) increases when the pressure gradient increases.

The organization of the paper is as follows: In Section 2 we introduce the problem and record the governing equations and the boundary conditions. In Section 3, we derive the non-dimensional

equations that govern the flow, and this is followed by Section 4 where we discuss the numerical solution to the problem on hand and make some concluding remarks. Some suggestions for future work are summarized in Section 5 and a brief description of the finite element scheme used for the computational resolution of the problem is given in Appendix A.

2. Governing equations

The equations governing the flow of a fluid through a porous solid can be derived systematically within the context of the theory of mixtures (see Truesdell [29, 30], Atkin and Craine [31, 32], Bowen [33], Rajagopal and Tao [34]). We shall not derive the equation from scratch, here, we refer the reader to Rajagopal [3] where a derivation is provided. The assumption that the viscosity of the fluid depends on the pressure and that the frictional effects in the fluid are not ignored implies that the Cauchy stress $\boldsymbol{T}$ in the fluid is given by

$$\boldsymbol{T} = -p\mathbf{1} + 2\mu(p)\boldsymbol{D}, \tag{2.1}$$

where $-p\mathbf{1}$ is the indeterminate part of the stress due to the constraint of incompressibility, $\boldsymbol{v}$ is the velocity of the fluid, $\mu(p)$ is the pressure dependent viscosity and $\boldsymbol{D}$ denotes the symmetric part of the velocity gradient, i.e.,

$$\boldsymbol{D} := \frac{1}{2}\left[\left(\frac{\partial \boldsymbol{v}}{\partial \boldsymbol{x}}\right) + \left(\frac{\partial \boldsymbol{v}}{\partial \boldsymbol{x}}\right)^{T}\right]. \tag{2.2}$$

The balance of linear momentum for the fluid, on neglecting body forces, is given by

$$\rho\frac{d\boldsymbol{v}}{dt} = \operatorname{div}[\boldsymbol{T}] + \boldsymbol{I}, \tag{2.3}$$

where $\boldsymbol{I}$ is the interaction between the solid and the fluid, namely the frictional resistance at the pores of the solid on the fluid that is flowing.

In general, there could be various other interaction mechanisms: drag, virtual mass effect, Magnus effect, Basset forces, Faxen forces, density gradient effects, temperature gradient effects, etc. We shall assume that the only interaction mechanism is that due to drag and that $\boldsymbol{I}$ is given by

$$\boldsymbol{I} = -\alpha(p)\boldsymbol{v}. \tag{2.4}$$

Since we shall be interested in slow flow, inertial effects in (2.3) are neglected. Also, since we shall assume that the fluid is incompressible, the velocity field has to satisfy the constraint that

$$\operatorname{div}[\boldsymbol{v}] = 0. \tag{2.5}$$

It follows from (2.1)–(2.4), on neglecting the inertial term that the appropriate governing equation is

$$-\frac{\partial p}{\partial \boldsymbol{x}} + \operatorname{div}[2\mu(p)\boldsymbol{D}] - \alpha(p)\boldsymbol{v} = \mathbf{0}. \tag{2.6}$$

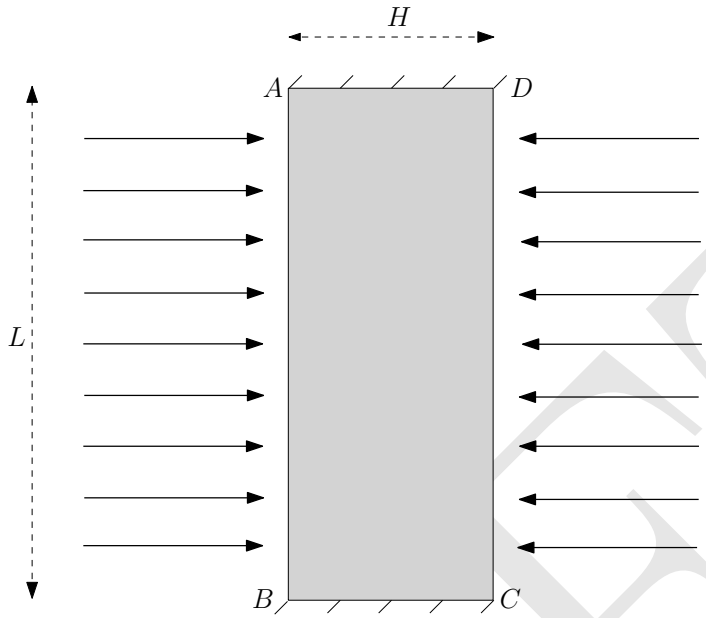

FIGURE 1. Pressure driven flow through a slab of length L and width H. A purely normal traction is applied at the left and right boundaries. The fluid satisfies no-slip boundary condition at the top and bottom of the slab

We shall be interested in the flow in a slab [2] due to the applied tractions on the surfaces AB and CD, that is,

$$\boldsymbol{t}\Big|_{AB} = [-p\mathbf{1} + 2\mu(p)\boldsymbol{D}]\Big|_{AB}\boldsymbol{n}_{AB}, \tag{2.7a}$$

$$\boldsymbol{t}\Big|_{CD} = [-p\mathbf{1} + 2\mu(p)\boldsymbol{D}]\Big|_{CD}\boldsymbol{n}_{CD}, \tag{2.7b}$$

where $\boldsymbol{n}_{AB}$ and $\boldsymbol{n}_{CD}$ denote the outward unit normals on the surface AB and CD (see Figure 1). It is important to recognize that the traction boundary conditions not only take into account the appropriate pressure, they also take into account the appropriate components of the velocity gradient. In addition to the above boundary conditions on the surface AB and CD, we assume that on the surface BC and AD, the fluid satisfies the no-slip boundary condition, i.e.,

$$\boldsymbol{v}\Big|_{BC} = \boldsymbol{v}\Big|_{AD} = \mathbf{0}. \tag{2.8}$$

Thus we need to solve (2.6) subject to the boundary conditions (2.7) and (2.8).

It must be remembered that classical solutions are not possible even in the case of linear partial differential equations unless the boundary data satisfy certain compatibility conditions (see [36]).

[2] A similar problem was studied by Subramanian and Rajagopal [35]. However a semi-inverse method was employed in that study which simplified the problem to a unidirectional flow across the slab. Here, we solve the system of partial differential equations that allows for flow along the direction of the pressure gradient as well as normal to it.

Such is the case in the present work, for the chosen values of the applied traction on AB and CD lead to an incompatibility at the corners. This leads to sharp gradients and concomitant numerical difficulties in solving the discretized system of non-linear algebraic equations and the incompatibility of the boundary conditions leads to singularity at the boundary that leads to the spike in the pressure that is observed in the numerical solution that we have obtained.

It is worth observing that when the viscosity and the "Drag coefficient" are independent of the pressure, we recover the classical Brinkman equation. If the frictional effects within the fluid are ignored, we obtain the equations considered by Nakshatrala and Rajagopal [25], which is the generalization of Darcy's equation for a pressure dependent "Drag coefficient" . Equation (2.6) can be generalized to

$$-\frac{\partial p}{\partial \boldsymbol{x}} + \operatorname{div}[2\mu(p)\boldsymbol{D}] - \alpha(\|\boldsymbol{v}\|)\boldsymbol{v} = \boldsymbol{0}, \tag{2.9}$$

which is the generalization of (2.6) to include a Forchheimer like term (see Forchheimer [37]). A generalization of the Brinkman model to describe power law fluids has been considered in [38] and [39].

3. Non-dimensional equations

In order to carry out a systematic study we shall appropriately non-dimensionalize the governing equations. Let us suppose that the surface CD is exposed to the atmosphere so that the pressure (the mean normal stress) is the atmospheric pressure p_0. We introduce the following non-dimensionalization

$$\bar{p} := \frac{p}{p_0},\ \bar{\boldsymbol{x}} := \frac{\boldsymbol{x}}{H},\ \bar{\beta} := \frac{\beta}{\frac{1}{p_0}},\ \bar{\boldsymbol{v}} := \frac{\boldsymbol{v}}{v_0}, \tag{3.1}$$

where H is the thickness of the slab (see Figure 1) and v_0 is a representative velocity, say

$$v_0 := \frac{p_0}{\alpha_0 H}. \tag{3.2}$$

Also, let

$$\bar{\mu} := \frac{\mu}{\mu_0},\ \bar{\alpha} := \frac{\alpha}{\alpha_0}. \tag{3.3}$$

The following non-dimensional counterpart of (1.1)

$$\bar{\mu}(\bar{p}) = \bar{\alpha}(\bar{p}) = \begin{cases} \exp(\bar{\beta}\bar{p}) & \text{if } \bar{p} > 0, \\ 1 & \text{if } \bar{p} \leq 0, \end{cases} \tag{3.4}$$

is evidently a continuous function of the pressure. However, the function in (3.4) is not differentiable in the classical sense, and we postpone to Appendix A the description of the numerical method.

It follows from (3.1)–(3.4) that (2.6) can be expressed as

$$-\bar{\text{grad}}[\bar{p}] - \bar{\alpha}(\bar{p})\bar{\boldsymbol{v}} + \frac{1}{\mathcal{A}}\bar{\text{div}}[2\bar{\mu}(\bar{p})\bar{\boldsymbol{D}}] = \boldsymbol{0}, \tag{3.5a}$$

$$\bar{\text{div}}[\bar{\boldsymbol{v}}] = 0, \tag{3.5b}$$

where $\bar{\text{grad}}[\cdot] := \dfrac{\partial(\cdot)}{\partial\bar{\boldsymbol{x}}}$, $\bar{\text{div}}[\cdot] := \text{tr}[\bar{\text{grad}}[\cdot]]$, $\bar{\boldsymbol{D}} := \dfrac{1}{2}\left[\left(\dfrac{\partial\bar{\boldsymbol{v}}}{\partial\bar{\boldsymbol{x}}}\right) + \left(\dfrac{\partial\bar{\boldsymbol{v}}}{\partial\bar{\boldsymbol{x}}}\right)^T\right]$ and $\mathcal{A} := \dfrac{\alpha_0 H^2}{\mu_0}$ is a non-dimensional number that is the ratio of the frictional effect due to drag (frictional effect between the fluid and the pores in the solid) to the frictional effect within the fluid due to viscosity. We shall also find it convenient to introduce two additional non-dimensional numbers

$$\gamma := \frac{L}{H}, \quad P := \frac{p_{AB}}{p_0}. \tag{3.6}$$

The non-dimensional forms of the traction boundary conditions are then

$$\bar{\boldsymbol{t}}\Big|_{\bar{x}=1} = -1\mathbf{i}, \tag{3.7a}$$

$$\bar{\boldsymbol{t}}\Big|_{\bar{x}=0} = P\mathbf{i}, \tag{3.7b}$$

while the corresponding non-dimensional form of the no-slip boundary condition is

$$\bar{\boldsymbol{v}}\Big|_{\bar{y}=0} = \bar{\boldsymbol{v}}\Big|_{\bar{y}=\gamma} = \boldsymbol{0}. \tag{3.8}$$

The domain and the boundary conditions for (3.5) that we shall work with are illustrated in Figure 2.

Thus we solve (3.5) with the form for $\bar{\mu}, \bar{\alpha}$ given by (3.4) subject to the boundary conditions (3.7) and (3.8).

4. Numerical results

The various parameters in the problem were chosen as follows: We let $\alpha_0 = \mu_0 = 1$ and set $H = 1, L = 10$. This in conjunction with $p_0 = 10^5$ yields $\gamma = 10$, $\mathcal{A} = 1$. The traction at the left end is varied by varying P. From the experiments reported in [40, 41, 42] the measured value of the reciprocal of the pressure-viscosity exponent β is seen to lie in the range $30 - 100$ MPa for the fluids measured. Hence we choose to study the cases $\beta = 0, 1\times10^{-8}, 2\times10^{-8}, 3\times10^{-8}$ and 3.5×10^{-8} (in units of Pa^{-1}) which give a qualitative picture of the effects of pressure dependent viscosity over the range of measured values of the exponent β. The case $\beta = 0$ corresponds to the case of constant viscosity (or the standard Brinkman model). The values chosen for β lead to values of $\bar{\beta} = 0, 1\times10^{-3}, 2\times10^{-3}, 3\times10^{-3}$ and 3.5×10^{-3}. We allow P to take on the values $1, 100, 200, 300, 400$ and 500.

Note that the traction is specified at $\bar{x} = 0$ and $\bar{x} = 1$ and no-slip boundary condition is enforced at $\bar{y} = 0$ and $\bar{y} = 10$ including the corners.

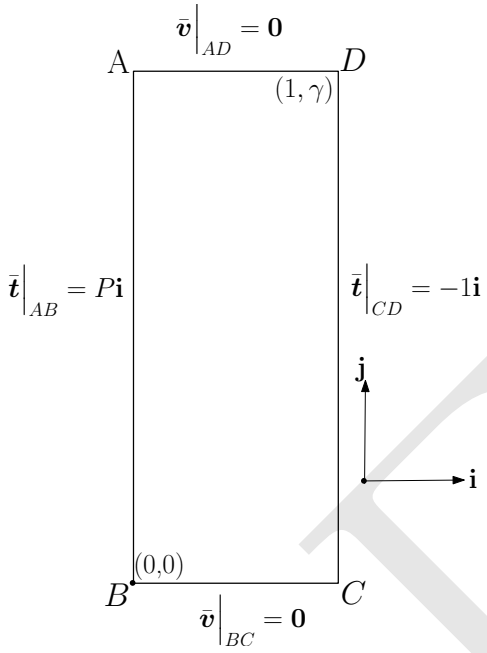

FIGURE 2. Pressure driven flow through a slab of length γ and width 1 with boundary conditions indicated on all sides of the slab.

We shall find it convenient to represent $\bar{\boldsymbol{v}}$ as

$$\bar{\boldsymbol{v}} = \bar{V}_x \mathbf{i} + \bar{V}_y \mathbf{j}. \tag{4.1}$$

A quantity of interest in this problem is the flux or flow rate obtained at the end of the slab that is open to the atmosphere, i.e., the side CD. We denote the non-dimensional flux by $\bar{q}$, where

$$\bar{q} := \int_{CD} [\bar{\boldsymbol{v}} \cdot \boldsymbol{n}_{CD}] \, \mathrm{d}l = \int_0^\gamma \bar{V}_x(1, \bar{y}) \mathrm{d}\bar{y}. \tag{4.2}$$

The system of (non-dimensionalized) partial differential equations (3.5) with the form for $\bar{\mu}, \bar{\alpha}$ given by (A.3) subject to the boundary conditions (3.7) and (3.8) was solved using a mixed finite element method, details of which are provided in the Appendix A.

The profiles of $\bar{V}_x$ and $\bar{p}$ at AB are shown in Figure 5 while the profiles at CD are shown in Figure 4. The lack of smoothness near the corners is expected; there is an incompatibility at the corners due to the change from the specified value of traction at AB and CD to a no-slip boundary condition at BC and AD. One can also notice that the velocity for the constant viscosity case is almost 200 percent more than that for the variable viscosity case

The contours of velocity and pressure over the entire domain are indicated in Figure 3. The contours of $\bar{V}_y$ indicate that unidirectional flow occurs only in a small region close to the middle of the slab. The pressure does not vary too much over the domain except for the occurrence of high pressures at some points close to the boundaries.

The variation of flux for different forcing pressures is shown in Figure 6. This is of great import because one observes that a standard Brinkman model with constant viscosity grossly overpredicts the flux; by as much as almost 250 percent for a pressure difference across the slab equal to 499 (which occurs when $P = 500$); the over prediction increases nearly linearly as can be seen from the figure. Also, the figure indicates that for the value of $\bar{\beta} = 3.5 \times 10^{-3}$, there is very negligible increase in the flux for forcing pressures $P > 200$, that is there seems to be a ceiling flux as is to be expected on physical grounds. This is in direct contrast to the case where the viscosity is constant and the model predicts a flux that will increase continuously with increase in P.

5. Conclusions and future work

The physical problem that pertains to enhanced oil recovery or carbon sequestration has several features that demand study in order to develop numerical techniques that can tackle the exponential variation in the viscosity and "Drag coefficient" with respect to the pressure. The boundary value problem considered here was merely a first step in the direction of solving a boundary value problem on a realistic flow domain that corresponds to practical problems.

From the point of view of modeling the physical phenomena, there are several issues that cry out for attention. Prominent amongst these are the following facts that need to be addressed:

(1) We do not have a single fluid but rather a mixture of two fluids: steam and oil. Thus we need to develop models that can adequately capture the interaction between the constituents. A study similar to this for a mixture of two incompressible fluids would be a noteworthy first step in this direction.
(2) The porous solid in reality is not rigid, it deforms due to the flow of the fluid through it. As a first approximation one could model the solid as a linearized elastic solid and then study a boundary value problem. Of course the question of appropriate boundary conditions for such problems is of great interest in its own right.
(3) In general it might be necessary to take into account the fact that the fluid in question is shear thinning. This would lead both the viscosity and the drag coefficient to depend on the shear rate (or to be precise the second principal invariant of the symmetric part of the velocity gradient).

A long-term goal would be to eventually allow the solid to fracture due to the applied pressure and model the hydraulic fracturing of the linearized elastic solid due to flow of a mixture of fluids through it.

Appendix A. Numerical Method

In this section we provide a short description of the finite element scheme that was used to obtain the numerical results.

Let $\Omega \subset \mathbb{R}^d$ be a non-dimensionalized open bounded domain, where $d = 2, 3$ is the number of spatial dimensions. The boundary $\partial\Omega$ is assumed to be Lipschitz continuous and is divided into two complementary parts $\Gamma^v \cap \Gamma^t = \emptyset$ and $\Gamma^v \cup \Gamma^t = \partial\Omega$. The part Γ^v is the part of the boundary on which the velocity is prescribed and is assumed to have non-zero measure while Γ^t is the part of the boundary on which the traction $\bar{\boldsymbol{t}}$ is imposed.

In order to write equations (3.5) in a weaker form suitable for continuous finite element methods, we denote by $L^2(K)$ the space of square integrable function defined over $K = \Omega$ or $K = \Gamma^t$

$$H^1(\Omega)^d := \left\{ \bar{\boldsymbol{v}} \in L^2(\Omega)^d \,\middle|\, \frac{\partial \bar{\boldsymbol{v}}}{\partial \bar{\boldsymbol{x}}_i} \in L^2(\Omega)^d,\ i = 1, ..., d \right\} \text{ and}$$
$$H^1_0(\Omega)^d := \left\{ \bar{\boldsymbol{v}} \in H^1(\Omega)^d \,\middle|\, \bar{\boldsymbol{v}} = 0 \text{ on } \Gamma^v \right\}.$$

We are now in position to write a weak formulation of (3.5): Given $\bar{\boldsymbol{t}} \in L^2(\Gamma^t)$, find $\bar{\boldsymbol{v}} \in H^1_0(\Omega)^d$ and $\bar{p} \in L^2(\Omega)$ such that for all $(\boldsymbol{w}, q) \in H^1_0(\Omega)^d \times L^2(\Omega)$

$$\int_\Omega \bar{\alpha}(\bar{p})\bar{\boldsymbol{v}} \cdot \boldsymbol{w} - \int_\Omega \bar{p}\ \bar{\mathrm{div}}[\boldsymbol{w}] + \frac{2}{\mathcal{A}} \int_\Omega \bar{\mu}(\bar{p})\bar{\boldsymbol{D}} \cdot \bar{\mathrm{grad}}[\boldsymbol{w}] - \int_\Omega \bar{\mathrm{div}}[\bar{\boldsymbol{v}}]\ q = \int_{\Gamma^t} \bar{\boldsymbol{t}} \cdot \boldsymbol{w}, \tag{A.1}$$

where the " $\cdot$ " denotes the standard inner product for vectors or tensors (that will be clear from the context). A corresponding conforming finite element formulation reads: Given $\bar{\boldsymbol{t}} \in L^2(\Gamma^t)$, find $\bar{\boldsymbol{v}}_h \in \mathcal{V}_h$ and $\bar{p}_h \in \mathcal{Q}_h$ such that for all $(\boldsymbol{w}_h, q_h) \in \mathcal{V}_h \times \mathcal{Q}_h$

$$\int_\Omega \bar{\alpha}(\bar{p}_h)\bar{\boldsymbol{v}}_h \cdot \boldsymbol{w}_h - \int_\Omega \bar{p}_h\ \bar{\mathrm{div}}[\boldsymbol{w}_h] + \frac{2}{\mathcal{A}} \int_\Omega \bar{\mu}(\bar{p}_h)\bar{\boldsymbol{D}}_h \cdot \bar{\mathrm{grad}}[\boldsymbol{w}_h] - \int_\Omega \bar{\mathrm{div}}[\bar{\boldsymbol{v}}_h]\ q_h = \int_{\Gamma^t} \bar{\boldsymbol{t}} \cdot \boldsymbol{w}_h, \tag{A.2}$$

where $\bar{\boldsymbol{D}}_h := \dfrac{1}{2}\left[\left(\dfrac{\partial \bar{\boldsymbol{v}}_h}{\partial \bar{\boldsymbol{x}}} \right) + \left(\dfrac{\partial \bar{\boldsymbol{v}}_h}{\partial \bar{\boldsymbol{x}}} \right)^T \right]$ while $\mathcal{V}_h$ and $\mathcal{Q}_h$ are finite-dimensional subspaces of $H^1_0(\Omega)^d$ and $L^2(\Omega)$ respectively.

The *inf-sup* or LBB condition constrains the choice of the finite-dimensional spaces $\mathcal{V}_h$ and $\mathcal{Q}_h$ for finite element formulations (A.2) to be suitable approximations of (A.1). In particular, equal-order interpolation for both pressure and velocity are not suitable (see [43]). Here the so-called *Taylor-Hood* combination is used. That is, after the domain is divided into a number of quadrilaterals when $d = 2$ or hexahedra when $d = 3$, on each element the pressure is approximated by a piecewise linear polynomial in each variable while the velocity is approximated by a piecewise quadratic polynomial in each variable, both approximations being globally continuous.

In this study, the rectangular domain was divided into 4×100 rectangles where the pressure was computed at the four corner nodes while the velocity was computed at nine nodes (four corners, four midpoints of sides, and the midpoint of diagonals). The mesh was made extremely fine (almost

10^{-11}) near the top and bottom in order to capture the steep gradients developed due to the boundary condition.

The resulting system of non-linear algebraic equations was solved by using a Newton-Raphson iteration algorithm in conjunction with a line search as outlined in [44]. The solution to $\bar{\beta} = 0$ was provided as an initial guess for $\bar{\beta} = 1 \times 10^{-3}$ and so on until the desired value of $\bar{\beta}$ was reached.

Note that the viscosity $\bar{\mu}$ and drag $\bar{\alpha}$ given by (3.4) are continuous but not differentiable. Hence in our numerical scheme we approximate it by the smooth function [3]

$$\bar{\mu}_h(\bar{p}) := \exp(\bar{\beta}\bar{p}) \cdot \tfrac{1}{2}\left[1 + \tanh\left(\frac{\bar{p}}{10h_{\min}}\right)\right] + 1 \cdot \tfrac{1}{2}\left[1 + \tanh\left(\frac{-\bar{p}}{10h_{\min}}\right)\right] =: \bar{\alpha}_h(\bar{p}) \tag{A.3}$$

where $h_{\min}$ represents the length of the smallest element in the mesh.

In the limit of mesh refinement, $\lim_{h\to 0} \bar{\mu}_h(\bar{p}) \to \bar{\mu}(\bar{p})$ and $\lim_{h\to 0} \bar{\alpha}_h(\bar{p}) \to \bar{\alpha}(\bar{p})$ where $\bar{\mu}(\bar{p})$ and $\bar{\alpha}(\bar{p})$ are as in (3.4), so our approximation is verified to be consistent.

Acknowledgments

S. Shriram and K. R. Rajagopal gratefully acknowledge the support from the Texas Engineering Experiment Station. A. Bonito thanks the King Abdullah University of Science and Technology (KAUST) for its award KUS-C1-016-04 in support of this work, and K. R. Rajagopal thanks the Office of Naval Research for its support of this work.

References

[1] Henry Darcy. *Les Fontaines Publiques de la Ville de Dijon*. Victor Dalmont, Paris, 1856.

[2] D. Munaf, D. Lee, A. S. Wineman, and K. R. Rajagopal. A boundary value problem in groundwater motion analysis-comparisons based on Darcy's law and the continuum theory of mixtures. *Mathematical Modeling and Methods in Applied Science*, 3:231–248, 1993.

[3] K. R. Rajagopal. On a hierarchy of approximate models for flows of incompressible fluids through porous solids. *Mathematical Models and Methods in Applied Sciences*, 17:215–252, 2007.

[4] H. C. Brinkman. On the permeability of the media consisting of closely packed porous particles. *Applied Scientific Research*, A1:81–86, 1947.

[5] H. C. Brinkman. A calculation of the viscous force exerted by a flowing fluid on a dense swarm of particles. *Applied Scientific Research*, A1:27–34, 1947.

[6] P. W. Bridgman. *The Physics of High Pressure*. MacMillan Company, New York, USA, 1931.

[7] G. G. Stokes. On the theories of internal friction of fluids in motion and of the equilibrium and motion of elastic solids. *Transactions of Cambridge Philosophical Society*, 8:287–305, 1845.

[8] C. Barus. Isotherms, isopiestics and isometrics relative to viscosity. *American Journal of Science*, 45:87–96, 1893.

[9] E. N. da. C. Andrade. Viscosity of liquids. *Proceedings of the Royal Society of London, Series A*, 215:36–43, 1952.

[3] We are motivated by the fact that the Heaviside function $H(x)$ may be realized as the limit of a sequence of smooth functions, namely, $H(x) = \lim_{n\to\infty} \frac{1}{2}[1 + \tanh(nx)] = \lim_{n\to\infty} [1 + \exp(-2nx)]^{-1}$.

[10] K. R. Rajagopal. Rethinking the developments of constitutive relations. To appear.

[11] M. Paluch, Z. Dendzik, and S. J. Rzoska. Scaling of high-pressure viscosity data in low-molecular-weight glass-forming liquids. *Physical Review B*, 60(5):2979–2982, 1999.

[12] K. L. Johnson and J. L. Tevaarwerk. Shear behavior of elastohydrodynamic oil films. *Proceedings of the Royal Society of London Series A-Mathematical Physical and Engineering Sciences*, 356(1685):215–236, 1977.

[13] K. L. Johnson and J. A. Greenwood. Thermal-analysis of an Eyring fluid in elastohydrodynamic traction. *Wear*, 61(2):353–374, 1980.

[14] K. L. Johnson and R. Cameron. Shear behavior of elastohydrodynamic oil films at high rolling contact pressures. *Proc. Inst. Mech. Eng.*, 182(1):223–229, 1967.

[15] K. R. Harris and S. Bair. Temperature and pressure dependence of the viscosity of diisodecyl phthalate at temperatures between 0 and 100 degrees C and at pressures to 1 GPa. *Journal of Chemical and Engineering Data*, 52(1):272–278, 2007.

[16] E. M. Griest, W. Webb, and R. W. Schiessler. Effect of pressure on viscosity of higher hydrocarbons and their mixtures. *The Journal of Chemical Physics*, 29(4):711–720, 1958.

[17] W. G. Cutler, R. H. McMickle, W. Webb, and R. W. Schiessler. Study of the compressions of several high molecular weight hydrocarbons. *The Journal of Chemical Physics.*, 29(4):727–740, 1958.

[18] R. Casalini and S. Bair. The inflection point in the pressure dependence of viscosity under high pressure: a comprehensive study of the temperature and pressure dependence of the viscosity of propylene carbonate. *The Journal of Chemical Physics*, 128(8):1–7, 2008.

[19] J. T. Bendler, J. J. Fontanella, and M. F. Shlesinger. A new Vogel-like law: ionic conductivity, dialectric relaxation and viscosity near the glass transition. *Physical Review Letters*, 87(19):1–4, 2001.

[20] S. Bair and F. Qureshi. Ordinary shear-thinning and its effect upon EHL film thickness. In D. Dowson et al., editors, *Tribological Research and Design for Engineering Systems*, pages 693–699. Elsevier, Amsterdam, 2003.

[21] S. Bair and P. Kottke. Pressure-viscosity relationships for elastohydrodynamics. *Tribology Transactions*, 46(3):289–295, 2003.

[22] S. Bair, M. Khonsari, and W. O. Winer. High-pressure rheology and limitations of the Reynolds equation. *Tribology International*, 31(10):573–586, 1998.

[23] D. Dowson and G. R. Higginson. *Elastohydrodynamic Lubrication: The Fundamentals of Roller and Gear Lubrication*. Pergamon Press, Oxford, 1966.

[24] K. R. Rajagopal. A semi-inverse problem of flows of fluids with pressure-dependent viscosities. *Inverse Problems in Science and Engineering*, 16(3):269–280, 2008.

[25] K. B. Nakshatrala and K. R. Rajagopal. A numerical study of fluids with pressure dependent viscosity flowing through a rigid porous media. *International Journal for Numerical Methods in Fluids*, 67:342–368, 2009.

[26] K. Kannan and K. R. Rajagopal. Flow through porous media due to high pressure gradients. *Applied Mathematics and Computation*, 199:748–759, 2008.

[27] V. Girault, F. Murat, and A. Salgado. Finite element discretization of Darcy's equations with pressure dependent porosity. *ESAIM: Mathematical Modelling and Numerical Analysis*, 44(6):1155–1191, 2010.

[28] A. Z. Szeri. *Fluid Film Lubrication: Theory and Design*. Cambridge University Press, Cambridge, 1998.

[29] C. Truesdell. Sulla basi della thermomechanica. *Rendiconti dei Lincei*, 22:33–38, 1957.

[30] C. Truesdell. Sulla basi della thermomechanica. *Rendiconti dei Lincei*, 22:158–166, 1957.

[31] R. J. Atkin and R. E. Craine. Continuum theories of mixtures: Basic theory and historical development. *The Quaterly Journal of Mechanics and Applied Mathematics*, 29:209–244, 1976.

[32] R. J. Atkin and R. E. Craine. Continuum theories of mixtures: Applications. *The Quaterly Journal of Mechanics and Applied Mathematics*, 17:153–207, 1976.

[33] R. M. Bowen. Theory of mixtures. In A. C. Eringen, editor, *Continuum Physics*, volume III. Academic Press, New York, 1976.

[34] K. R. Rajagopal and L. Tao. *Mechanics of Mixtures*. World Scientific Publishing, River Edge, New Jersey, USA, 1995.

[35] S. C. Subramanian and K. R. Rajagopal. A note on the flow through porous solids at high pressures. *Computers and Mathematics with Applications*, 53:260–275, 2007.

[36] C. Miranda. *Partial differential equations of elliptic type*, volume 370. Springer-Verlag, Berlin, 1970.

[37] P. Forchheimer. Wasserbewegung durch Boden. *Zeitschrift des Vereines Deutscher Ingeneieure*, 45:1782–1788, 1901.

[38] Maria Laura Martins-Costa, Rogério M. Saldanha da Gama, and S. Frey. Modeling of a generalized Newtonian flow through channels with permeable wall. *Mechanics Research Communications*, 27(6):707–712, November-December 2000.

[39] Heraldo S. Costa Mattos, Maria Laura Martins-Costa, and Rogério M. Saldanha da Gama. On the modelling of momentum and energy transfer in incompressible mixtures. *International Journal of Non-linear Mechanics*, 30(4):419–431, 1995.

[40] Richard C. Penwell, Roger S. Porter, and Stanley Middleman. Determination of the pressure coefficient and pressure effects in capillary flow. *Journal of Polymer Science Part A-2: Polymer Physics*, 9(4):731–745, 1971.

[41] C. J. Schaschke, S. Allio, and E. Holmberg. Viscosity measurement of vegetable oil at high pressure. *Food and Bioproducts Processing*, 84(3):173–178, 2006.

[42] J. M. Paton and C. J. Schaschke. Viscosity measurement of biodiesel at high pressure with a falling sinker viscometer. *Chemical Engineering Research and Design*, 87(11):1520–1526, 2009.

[43] F. Brezzi and M. Fortin. *Mixed and Hybrid Finite Element Methods, volume 15 of Springer series in computational mathematics*. Springer-Verlag, New York, USA, 1991.

[44] William H. Press, Saul A. Teukolsky, William T. Vetterling, and Brian P. Flannery. *Numerical recipes: The Art of Scientific Computing*. Cambridge University Press, New York, 2007.

[45] John D. Hunter. Matplotlib: A 2D Graphics Environment. *Computing in Science & Engineering*, 9(3):90–95, May-Jun 2007.

[46] Tecplot. *Tecplot 360: User's Manual*. URL: http://www.tecplot.com, Bellevue, Washington, USA, 2011.

[47] Otfried Schwarzkopf. The Extensible Drawing Editor Ipe. In *Proceedings of the Eleventh Annual Symposium on Computational Geometry*, SCG '95, pages 410–411, New York, NY, USA, 1995. ACM.

Department of Mathematics, Texas A&M University, College Station, Texas 77843.
E-mail address: bonito@math.tamu.edu

Department of Mechanical Engineering, Texas A&M University, College Station, Texas 77843.
E-mail address: krajagopal@tamu.edu

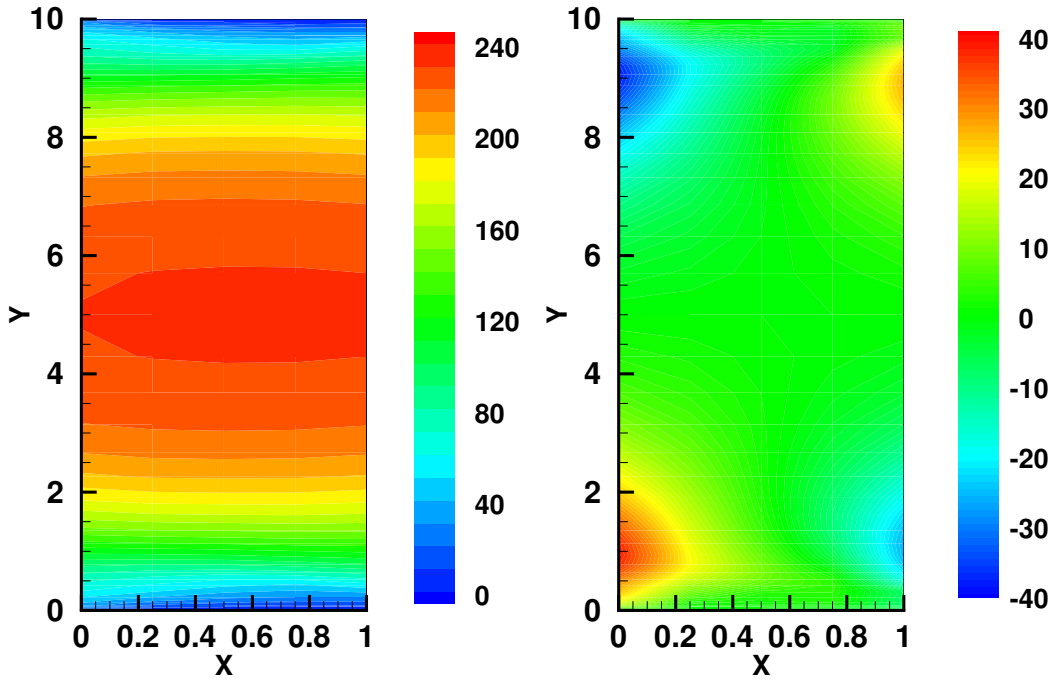

(A) $\bar{V}_x$ (B) $\bar{V}_y$

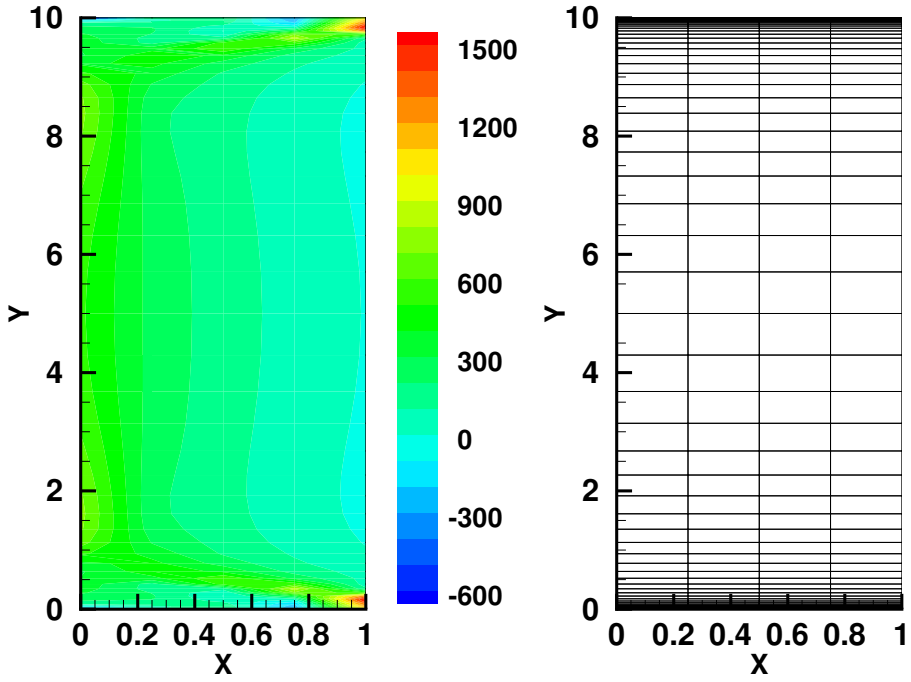

(C) $\bar{p}$ (D)

FIGURE 3. Contours of velocity and pressure for $\bar{\beta} = 3.5 \times 10^{-3}$ when $P = 500$. The finite element mesh used is also shown.

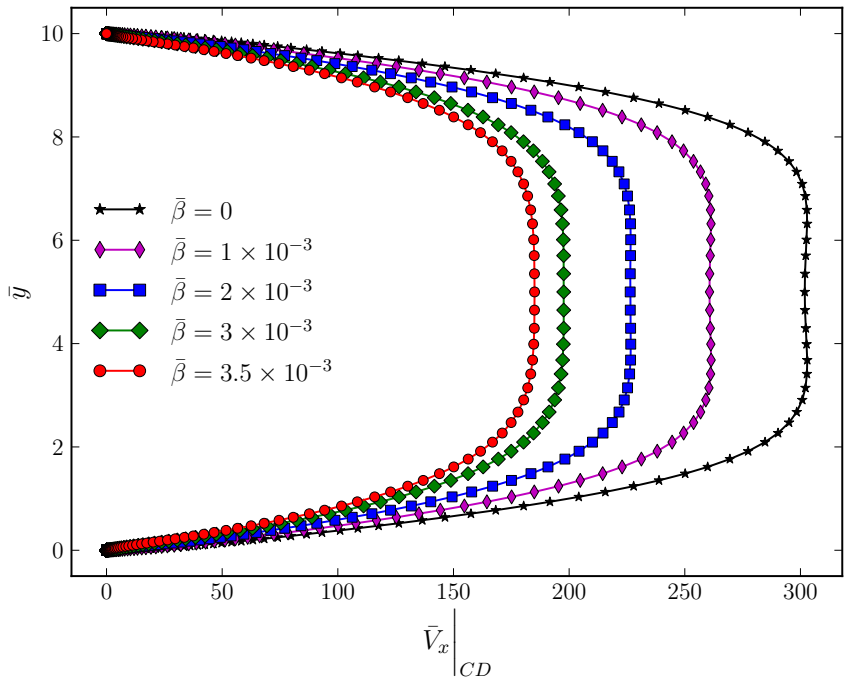

(A)

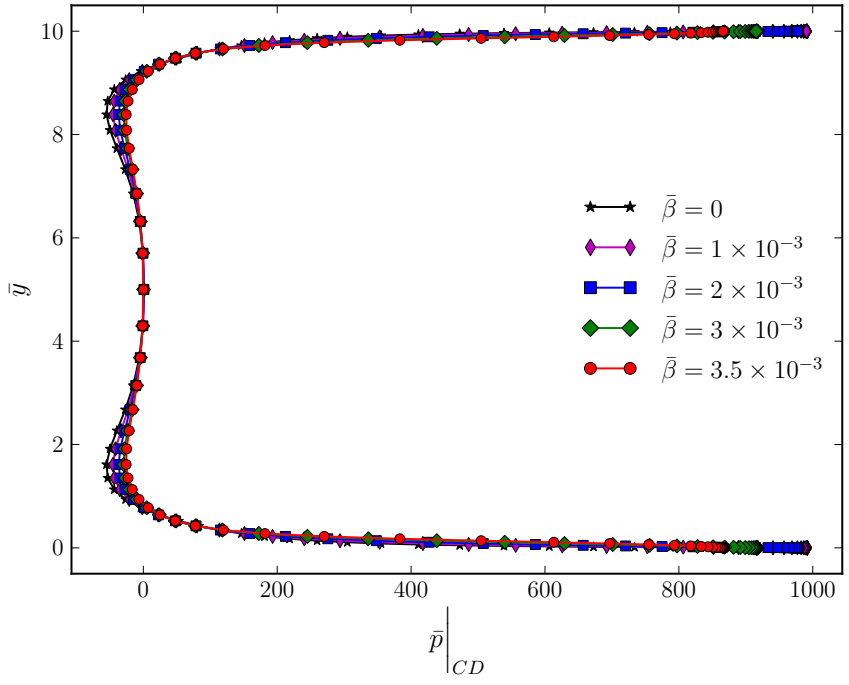

(B)

FIGURE 4. Velocity and pressure profiles at the right end $\bar{x} = 1$ with $P = 300$ for various $\bar{\beta}$.

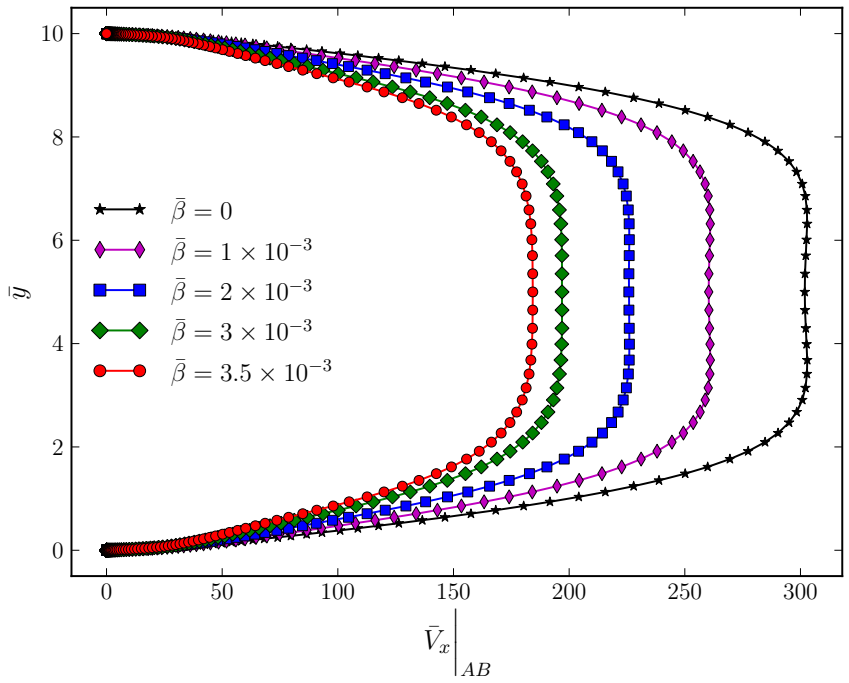

(A)

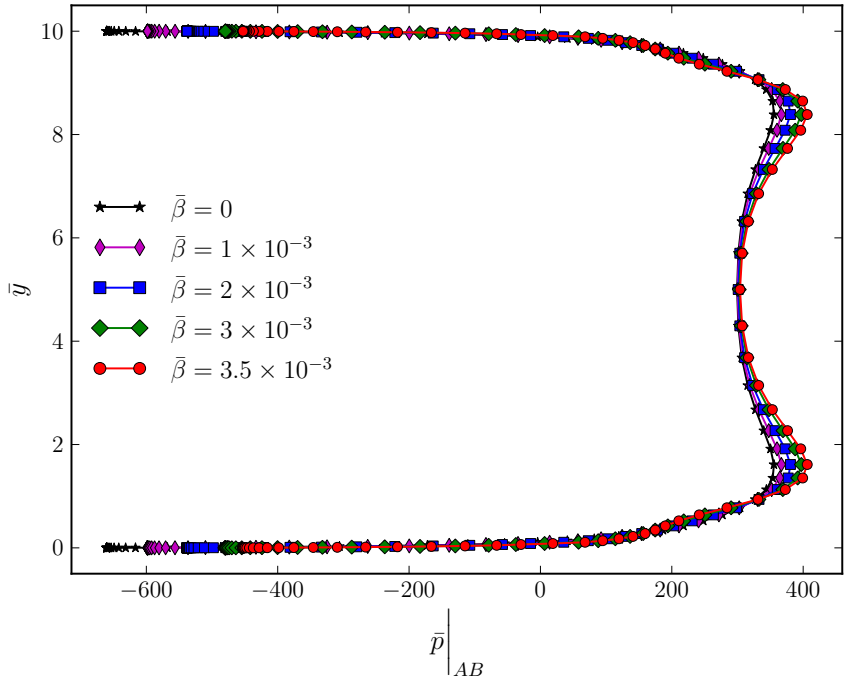

(B)

FIGURE 5. Velocity and pressure profiles at the left end $\bar{x} = 0$ with $P = 300$ for various $\bar{\beta}$.

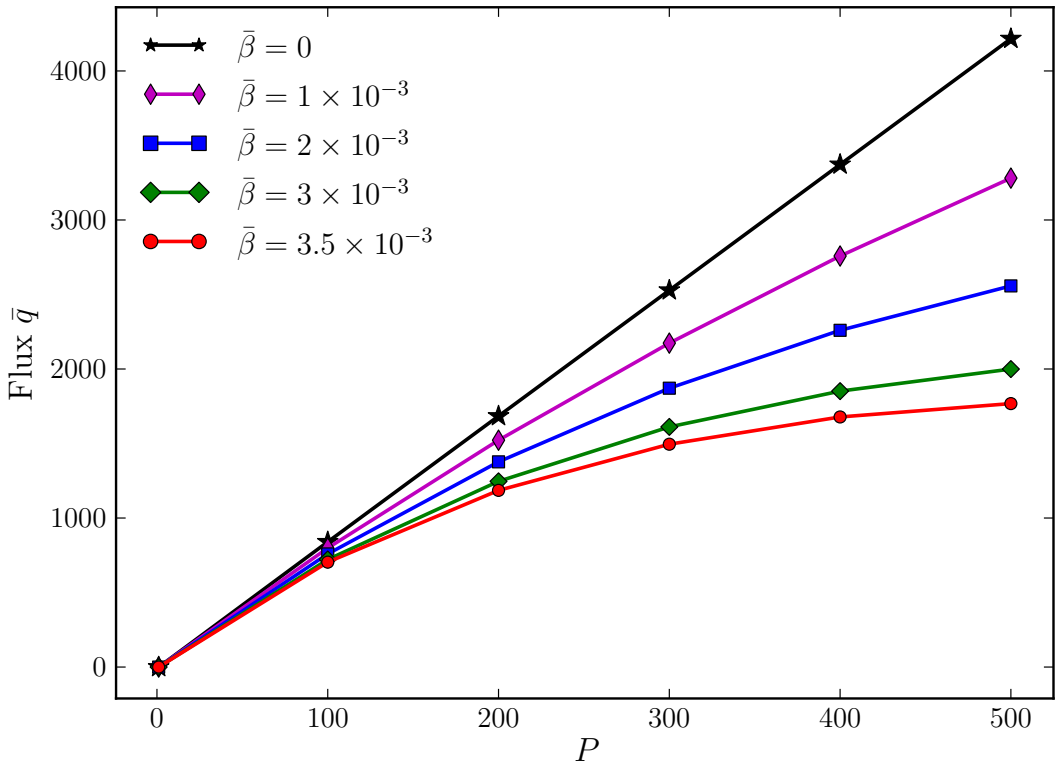

FIGURE 6. Flow rate through the slab for different values of traction at the left boundary